

AperTO - Archivio Istituzionale Open Access dell'Università di Torino

The CNAO dose delivery system for modulated scanning ion beam radiotherapy

This is a pre print version of the following article:

Original Citation:

Availability:

This version is available <http://hdl.handle.net/2318/158027> since 2017-05-28T18:19:48Z

Published version:

DOI:10.1118/1.4903276

Terms of use:

Open Access

Anyone can freely access the full text of works made available as "Open Access". Works made available under a Creative Commons license can be used according to the terms and conditions of said license. Use of all other works requires consent of the right holder (author or publisher) if not exempted from copyright protection by the applicable law.

(Article begins on next page)

The CNAO Dose Delivery System for ion pencil beam scanning radiotherapy

S. Giordanengo^{a)}, M. A. Garella^{a,b)}, F. Marchetto^{a)}, F. Bourhaleb^{a,c)*},
5 M. Ciocca^{b)}, A. Mirandola^{b)}, M. A. Hosseini^{a,c)}, C. Peroni^{a,c)}, R.
Sacchi^{a,c)}, R. Cirio^{a,c)} and M. Donetti^{a,b)}

a) Istituto Nazionale di Fisica Nucleare, Section of Torino, 10125
Torino, Italy;

10 b) Centro Nazionale Adroterapia Oncologica, 27100 Pavia, Italy;

c) University of Torino, Physics Department, 10125 Torino, Italy;

*) Now at I-see srl, 10125 Torino, Italy

Abstract

15 **Purpose:** This paper describes the system for the dose delivery
currently used at the Centro Nazionale di Adroterapia
Oncologica (CNAO) for ion pencil beam scanning
radiotherapy.

Methods: CNAO Foundation, Istituto Nazionale di Fisica
20 Nucleare (INFN) and University of Torino have designed, built
and commissioned a Dose Delivery System (DDS) to guide ion
beams accelerated by a dedicated synchrotron and to distribute
the dose with a full 3D scanning technique. Protons and carbon
ions are provided for a wide range of energies in order to cover
25 a sizeable span of treatment depths.

The target volume, segmented in several layers orthogonally to the beam direction, is irradiated by thousands of pencil beams which must be steered and held to the prescribed positions until the prescribed number of particles has been delivered. For the
30 CNAO beam lines these operations are performed by the DDS. The main components of this system are two independent beam monitoring systems, BOX1 and BOX2, and two control systems, performing of the tasks of real-time fast and slow control, which in turn are interfaced with the scanning magnets
35 and the beam chopper. The essential tasks and operations are described following the data flow from the Treatment Planning System (TPS) down to the end of the treatment delivery. As a reaction to any condition leading to a potential hazard, a DDS interlock signal is sent to the Patient Interlock System which
40 immediately stops the irradiation.

Results: The ability of the DDS to guarantee a safe and accurate treatment was validated during the commissioning phase by means of checks of the charge collection efficiency, gain uniformity of the integral chambers and 2D dose
45 distribution homogeneity and stability. A high level of reliability and robustness has been verified in the two years of activity with 100% up-time of the system. Four identical DDS devices showing comparable performances have been tested on the CNAO beam lines and are presently in use for clinical
50 activity.

Conclusions: The Dose Delivery System described in this paper is one among the few existing systems worldwide to operate ion pencil beam scanning radiotherapy. At the time of writing it has been used to treat more than 200 patients and it
55 has proven to guide and control the therapeutic pencil beams with a high level of reliability, reaching performances well above clinical requirements in terms of dose accuracy and stability.

60 I. INTRODUCTION

Radiation therapy aims to deliver the prescribed amount of dose to the tumour sparing at the same time the surrounding tissues as much as possible. Radiation therapy with charged hadrons has been proposed as an option for patients for whom traditional treatment with photons is not expected to give the desired results. The interaction
65 properties of charged particles with matter lead to a dose deposition highly peaked at end of the range, the Bragg peak, where carbon ions feature an increased radiobiological effectiveness (RBE). These are the main reasons for exploiting charged hadrons in radiotherapy.

The pioneer passive beam delivery systems [1, 2, 3] are being replaced by active
70 systems [4, 5, 6, 7] which provide highly conformal dose distributions using pristine monoenergetic pencil beams at well-defined penetration depths without any need for patient-specific hardware. The scanned ion beam technique is currently used only in few centers worldwide [8, 9, 10], but several existing and proposed facilities are developing scanning capabilities in Asia, Europe, and USA [11, 12, 13].

75 The use of a synchrotron to accelerate ions in a wide range of energies results in a fully
active three-dimensional (3D) dose delivery. The target volume, segmented in several
layers orthogonal to the beam direction, is irradiated by the superposition of a sequence
of pencil beams, each delivering a defined number of particles at a specific position. In
order to perform such operations with a high precision, a dedicated fast, accurate and
80 redundant Dose Delivery System (DDS) is required. The DDS thus plays a crucial role
within the complex architecture of a hadrontherapy facility.

This paper provides a description of the DDS in use at Centro Nazionale di Adroterapia
Oncologica (CNAO), a hospital-based facility built in Pavia, Italy, to treat cancer using
beam scanning techniques and to perform advanced research in the fields of
85 hadrontherapy, radiobiology and physics [14]. CNAO started treating patients with
protons in September 2011 and one year later with carbon ions too. At the time of
writing 200 patients, mainly chordoma and chondrosarcoma or squamous cell
carcinoma located in head and neck or spine region, have been treated, 100 with protons
and 100 with carbon ions.

90

In section II an overview of the CNAO treatment system is presented with a brief
description of the synchrotron, followed by a summary of the beam delivery technique
together with the scanning elements characteristics in order to illustrate the role of the
DDS components and their interfaces. The technical details of the DDS are reported in
95 section III, while the description of the several tasks performed by the system can be
found in section IV. Finally, section V is devoted to the treatment safety issues with the
description of interlocks handling, while examples of the system performance are
reported in the last section (VI).

100 II. OVERVIEW OF THE CNAO TREATMENT SYSTEM

II.A Accelerator and beam characteristics

The CNAO synchrotron [14] has been designed to accelerate protons or carbon ions to energies corresponding to depth from 3 to 32 g/cm² and from 3 to 27 g/cm², respectively. Two identical ion sources, the radio frequency quadrupole and a linear
105 accelerator are located inside the 25 m diameter ring of the synchrotron. Particles are accelerated to the required energy by a radiofrequency cavity, which performs also the beam stabilization before extraction. Once the beam has been accelerated to the required energy, the extraction phase starts and particles are steered through the high energy beam transport line to the selected treatment room.

110 The period of the synchrotron cycle is typically between 4 and 5 s, where the spill length is approximately 1.5 s and the remaining time is used to setup the machine for the next spill.

The beam specifications are listed in Table 1. Changes of energy can be performed between spills and the number of particles delivered can be varied between 10¹⁰ protons
115 or 4×10⁸ carbon ions per spill down to approximately 10% of these values. The transverse beam dimensions vary for protons [carbon ions] from 20 mm [8 mm] FWHM at the lowest energy down to 7 mm [4 mm] at the highest energy. These figures are intended in air at the isocenter.

Maximum field size	20×20 cm ² at the isocenter
Beam range for protons/carbon ions	3÷32 gcm ⁻² /3÷27 gcm ⁻²
Beam energy range for protons/carbon ions	60÷250 MeV / 120÷400 MeV/u
min÷Max beam intensity for protons/carbon ions	10 ⁹ ÷10 ¹⁰ / 4×10 ⁷ ÷4×10 ⁸
Spot size (FWHM in air at the isocenter) protons/carbon ions	7÷20 /4÷8 mm from highest to lowest energies
Beam intensities	100 %, 50 %, 20 %,10%

Two treatment rooms are equipped with a fixed horizontal beam line, while in the third room both vertical and horizontal fixed lines are available. In the vertical line the beam is steered to the height of 4 m above the isocenter and then deflected to enter vertically the treatment room. Four identical Dose Delivery Systems, one for each beam line, are in use. A design of the room 2 with the horizontal and vertical beam lines is shown in Figure 1.

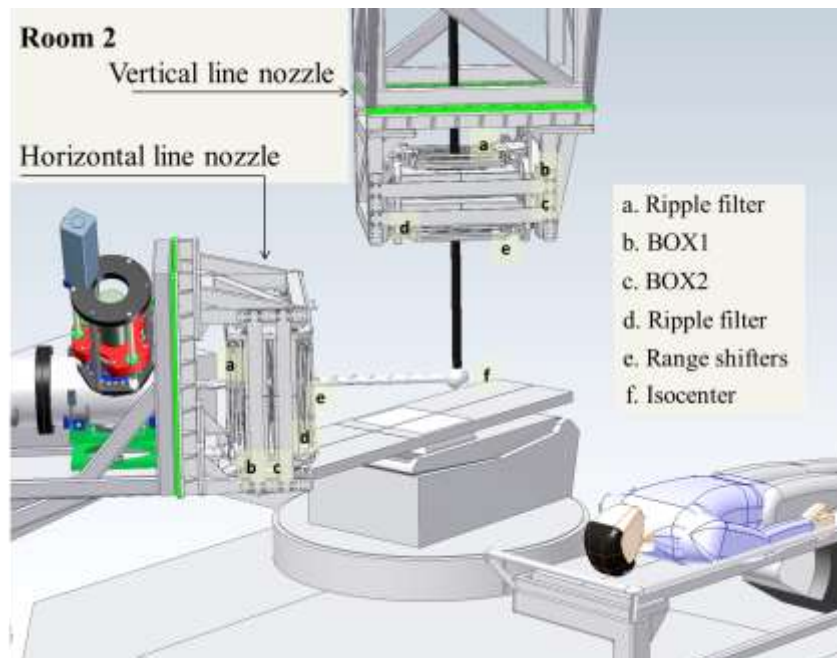


Fig. 1. Room 2 nozzles with horizontal and vertical beam lines: the particles reach the isocenter (f) going through a first ripple filter (a), the beam monitors (b BOX1, c BOX2), a second ripple filter (d), range shifters (e).

As shown in Figure 1 and 2, the elements placed downstream of the exit window are the beam monitors and a number of optional passive elements inserted to modify, if necessary, the longitudinal properties of the beam, as described in the following section.

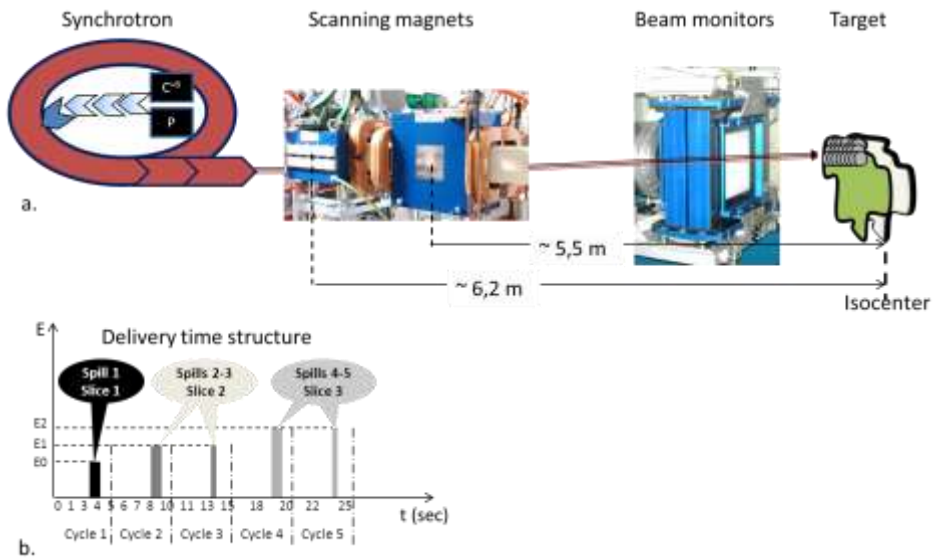


Fig. 2a. Scheme of the beam delivery technique with its main components (accelerator, scanning magnets, beam fluence and position monitors), with the 3-D target volume divided in iso-energy slices;

140 Fig. 2b. scheme of the delivery time structure subdivided in cycles.

For the horizontal lines a pair of dipole magnets, with orthogonally oriented fields, are used to deflect the beam horizontally (X) and vertically (Y), their centers being located at distances of 6.2m and 5.5 m upstream of the isocenter (Figure 2). A similar
 145 arrangement is used in the vertical line, with the steering magnets placed at a distance of 2.5 m and 2.0 m upstream of the 90° bending magnet.

II.B. Beam delivery

The dose delivered using the scanned ion beam technique results from the superposition of a large number of beams conveyed to the target. The irradiated volume is divided into
 150 several layers, called slices, orthogonal to the particle propagation direction [7]. Each layer is irradiated by several overlapping iso-energetic beams arranged in a grid of 2÷3 mm pitch, called spots, each delivering a dose in small volumes and characterized by the number of particles and by the position in the transverse plane. A typical treatment,

composed by more than 15÷20 daily fractions, each characterized by two or more fields
155 [15, 16], consists of 30 to 100 slices, for a total of 10000 to 50000 spots used to cover
the tumour volume.

Range shifters can be added to degrade the beam energy for shallow tumour treatments.
Furthermore for carbon ion beams it has to be underlined that Bragg peak is quite
narrow, when carbon ion beams are used. This would require the superposition of a too
160 large number of energies to achieve a uniform longitudinal dose distribution leading to
an inefficient use of the beam. This issue is solved by inserting up to two ripple filters to
broaden the pristine Bragg peak [17, 18]. During the treatment the DDS guides the
beam delivery irradiating the spots according to a sequence defined by the Treatment
Planning System (TPS). The number of particles delivered to a spot is measured by the
165 calibrated beam monitors and the beam is steered to the next spot acting on the scanning
magnets when the prescribed number of particles is reached. A tiny fraction of the dose
is therefore delivered between spots and the DDS includes this transient dose in the
arrival spot dose evaluation to prevent extra-dose. However, when distance between
spots centers is larger than a pre-defined threshold, the irradiation is paused.

170 This procedure is repeated until the last spot of the slice has been irradiated. The DDS
may require several identical spills to deliver the prescribed dose to a given slice. By
optimizing the number of particles in each spot [19] the dose to the target volume can be
precisely conformed to negligible water equivalent thickness crossed by the beam
before reaching the patient.

175 **II.C Magnetic scanning system**

One of the key elements of the pencil beam scanning technique is the complex of
steering magnets and power supplies [5, 9]. The details of construction and
performances are reported in [20] and references therein; here we give a short summary

180 focussing on the aspects which are more relevant to the DDS and the related clinical requirements.

The CNAO scanning magnets provide a $20 \times 20 \text{ cm}^2$ maximum clinical irradiation field corresponding to a maximum bending angle of 21 mrad. Particular care was taken in the design to achieve a uniform magnetic field over the full $12 \times 12 \text{ cm}^2$ aperture area in
185 addition to a low magnetic hysteresis. The power supplies feature a current sensitivity of 55 mA, which corresponds for the lowest beam energies to a 70 and 200 μm position sensitivity at the isocenter for carbon and proton beam respectively.

The other important design performance is the beam steering speed due to the fact that the beam is not stopped when moving from one position to the next. The magnetic
190 scanning system was carefully designed in order to minimize the transit time between spots which was measured to be less than 200 μs [20], corresponding to an average scanning speed exceeding 15 m/s. The relative effect on the dose depends on the time spent on each spot and on the beam intensity. However, as said before, the transient dose does not imply additional dose to the patient since it is accounted for by DDS as
195 part of the arrival spot.

III. THE CNAO DOSE DELIVERY SYSTEM

After a brief introduction on the roles of the DDS, a detailed description of the system is presented in three sections: components, tasks and operations, interlock management.

III.A. Introduction

200 The role of the DDS consists of delivering the dose according to the prescriptions, i.e. irradiating each spot with defined properties: number of particles, selected energy and specified position. The delivery needs to be performed ensuring the safety to the patient.

205 The above mentioned spot properties are provided as a DICOM RT file by the Syngo Siemens version VC10 TPS, which supports the delivery of both protons and carbon ions with scanning modality.

The patient related pre-treatment data flow starting from the TPS down to the synchrotron control and to the DDS is shown in Figure 3.

210

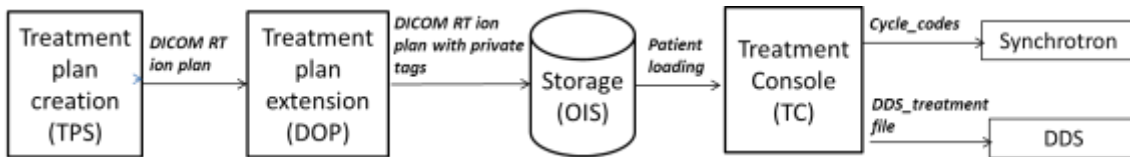


Fig. 3. Pre-treatment data flow starting from TPS down to, synchrotron control and the DDS through the Dicom Operating Powering (DOP), the Oncological Information System (OIS) and the Treatment Console (TC).

215

The DICOM Operating Powering (DOP) software tool adds information, stored in private DICOM tags, to the TPS plan in order to completely define the accelerator settings and to optimize the delivery. Among these, we mention optimization of the delivery path, instruction to switch-off the irradiation when large spot-to-spot distance

220 needs to be covered, selection of beam intensity and use of repainting techniques to

mitigate the effects of target motion. The extended treatment plan is stored in the Oncology Information System (OIS), Elekta Mosaiq version 2.50. Few minutes before the treatment starts, the Treatment Console (TC) receives the patient plan from OIS and sends to the accelerator control a list of binary codes (*cycle_codes*) defining the energy,

225 beam size, intensity and particle type for each spill. In parallel the *DDS_treatment* file,

containing the full list of spots grouped in slices (see Sec II.B), is produced and downloaded. The spot sequence defined in the *DDS_treatment* file is used by DDS during beam delivery to guide the beam during irradiation.

III.B. Dose Delivery System (DDS) components

230

The DDS components can be divided in two groups:

- beam detectors placed at the nozzle;
- control system.

III.B.1. Beam detectors

235

The DDS measures in time intervals the number of particles delivered, the beam position and the beam dimension by means of five parallel plate ionization chambers filled with nitrogen. The details of construction and performances are reported in [21] while a brief description is following. These monitors are enclosed in 2 independent

240

steel boxes: BOX1 and BOX2 (Figure 4). BOX1 contains an integral chamber (INT1) with a large area anode for the measurement of the beam fluence, integrated over the irradiation area, followed by two chambers with the anodes segmented in 128 strips, 1.65 mm wide, along with vertical (StripX) and horizontal (StripY) orientations, which provide the measurement of the beam position and beam width along the orthogonal directions. BOX2 contains a back-up integral chamber (INT2) followed by a chamber

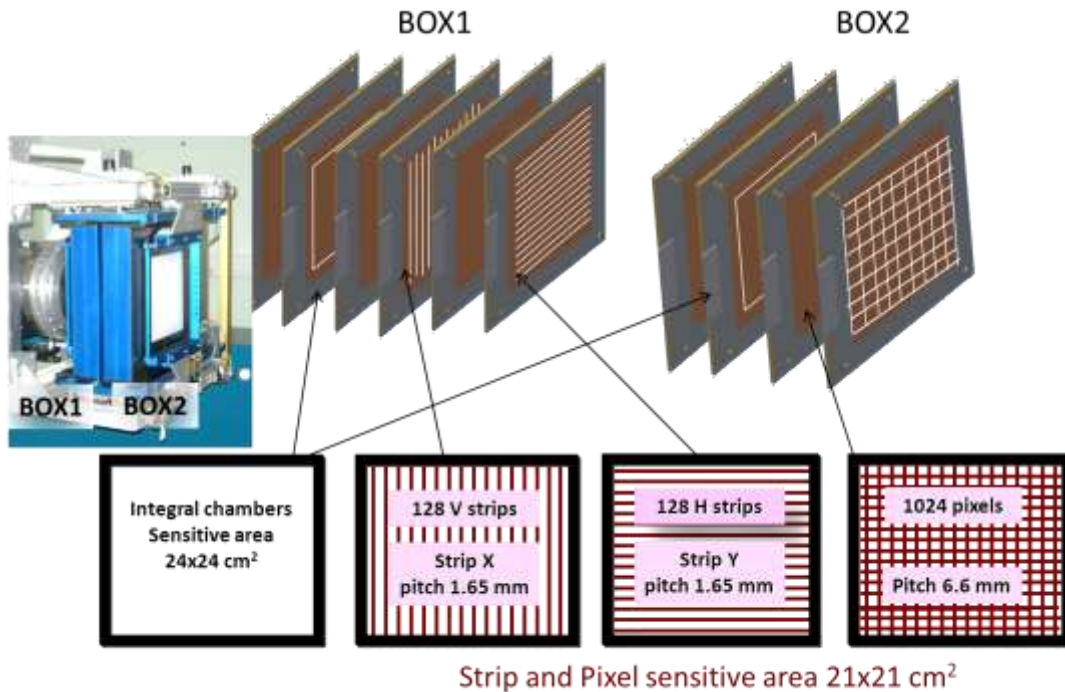
245

with the anode segmented in 32×32 pixels, 6.6 mm wide, (PIX). The measurements accomplished by BOX2 detectors are beam fluence, position and width.

The total water equivalent thickness of these chambers has been measured to be approximately 0.9mm. The material budget interposed by the beam detectors is spread along approximately 20 cm and it is one of the main contributors to the beam lateral

250

dispersion. To minimize the effect, the boxes are installed approximately 70 cm from the isocenter.



255 Fig. 4. Detail of the electrode segmentation for beam detectors (BOX1 and BOX2).

The detector front-end readout is based on custom designed boards, which host Application Specific Integrated Circuit electronics (ASIC) custom designed for this purpose. The chosen architecture and technology allows good sensitivity, with a
 260 minimum measured charged of 200 fC , that corresponds to 1.5×10^4 protons/ or 500 carbon ions. The background current is limited to 200 fA ; this ensures negligible over- or under- delivery of dose.

The customized electronics is based on large scale integration to provide many readout channels with uniform channel-to-channel behavior, and allow a large segmentation of
 265 the active area providing a good precision of the device.

The charge collected in the ionization chambers depends on the pressure and temperature of the gas, as well as on the high voltage across the gap. These quantities are monitored by a set of transducers installed in each box and controlled by a Peripheral Interface Controller (PIC). Values are periodically read and checked by the

270 PIC against pre-set values. The measured deviations are used to correct the gain of the
chambers. Appropriate interlock procedures are activated whenever any of the values is
not within the expected range (see Sec. III.B.2.2).

III.B.2. DDS control system

275 The control of the whole system that is detector power supplies, gas distribution,
interface with interlock system and dose delivered recovery system, are hosted in the
cabinet shown in Figure 5. To avoid as much as possible any radiation damage, it is kept
approximately two meters aside of the beam pipe, in a vault located right before the
treatment room and protected by a concrete wall.

280 The architecture of the system is based on commercial National Instruments (NI) crates
and boards. Two Peripheral Component Interconnect (PCI) eXtensions for
Instrumentation (PXI) crates are used: the Fast Control (FC), dedicated to the time
critical operations performed during the irradiation and the Slow Control (SC) to check
for the proper passive elements setup and for the system conditions before each
285 treatment.

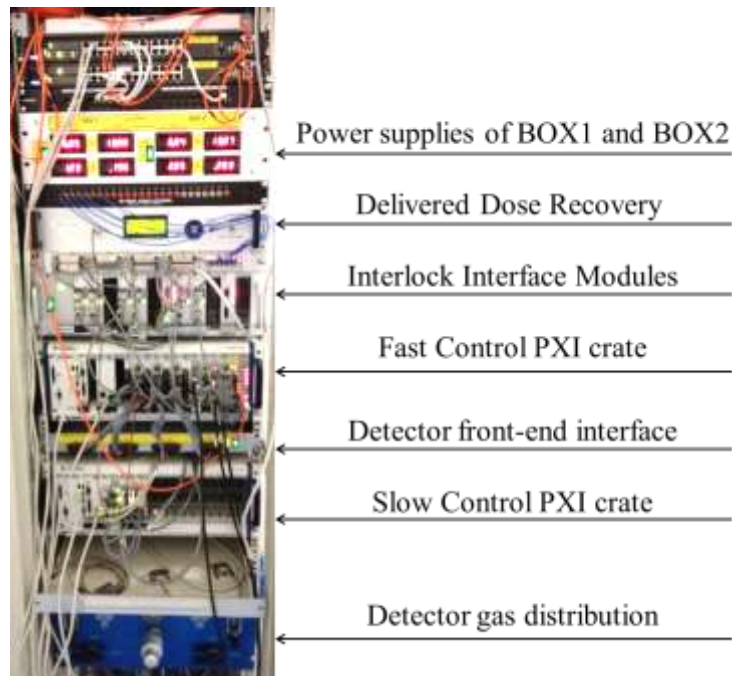


Fig. 5. Cabinet hosting the DDS.

290

III.B.2.1.Fast Control

The Fast Control crate includes a CPU running a Real-Time Operating System (RTOS), five NI PXI modules with Field Programmable Gate Array (FPGA) on board, four memory cards, one additional network card and three custom PXI modules.

295 The main intelligence and the safety of the DDS are entrusted into the 5 FPGAs which work in standalone mode to ensure maximum speed and reliability during the beam extraction phase.

While treating a spot, the leading role is played by the *Int FPGA*, which drives the delivery by sequentially accessing the prescribed spot properties, stored in the memory boards, and measuring the number of particles delivered through the integral ionization
 300 chambers (INT1 and INT2) at a sampling rate of 1 Msample/s. In parallel, the *Strip FPGA* and *Pixel FPGA* measure position and size of the pencil beam in the transversal plane through StripX, StripY and PIX detectors at a frequency of 20 kHz and 10 kHz respectively. A center of gravity algorithm is applied for beam position reconstruction

[21] as soon as a pre-defined minimum number of counts is reached in order to compare
305 the measured value with the planned one. The difference computed by the *Strip* FPGA
is used by the *Scan* FPGA to provide a feedback to the scanning magnets, which correct
for small position deviations. When the position deviations are larger than a threshold,
presently set at 2 mm, the *Strip* FPGA pauses the irradiation acting on the chopper.
When the hit strip does not reach a minimum number of counts, the feedback is
310 switched off and the position of the strip with largest number of counts is used.

The *Scan FPGA* is used to control the scanning magnets by sending the required current
to the power supplies and reading back the measured currents at a rate of 40 kHz. *Scan*
FGPA has also in charge to switch off the beam when the distance between spot centers
is greater than a threshold, (at present 20 mm), by acting on the beam chopper [14].

315 Finally the *Timing FPGA* interfaces the FC with the Master Timing Generator (MTG) to
synchronize the FC operations with the accelerator operations (magnet preparation,
beam acceleration, beam extraction, etc...). The MTG broadcasts *cycle_codes* (list of
binary codes, see section III.A) and synchrotron events to several systems and
equipment, (e. g. DDS) which need trigger signals from accelerator operation. Most of
320 the other systems read and use timing events, while DDS FC also generates and sends
events back to MTG itself. In particular, the FC at the end of each spill sends the events
Repeat_cycle or *Next_cycle* to ask for a new spill; this will coincide or not with the
previous one, depending if the slice has been completed (see section III.C). Additionally
the FC by means of the *Timing FPGA* grants the start of spill by replying to the MTG
325 the acknowledge of the *cycle_code* received.

III.B.2.2.Slow Control

The measurement of gas temperature and pressure inside the detectors and the control of
the high voltage applied to the chambers are important for accurate beam fluence

measurements. These controls are performed by the Slow Control (SC) system, which
 330 also checks for the passive elements setup (see section II.B). The SC crate includes one
 real-time CPU, three digital input-output cards, one additional network adapter, a serial
 card connected with the Slow Control system boards of BOX1 and BOX2 [21], and a
 PXI module to provide signals to the interlock system.

As described in Sec. II.B, range shifters and ripple filters may be needed for
 335 specific treatments. These elements are manually mounted and the setup verification is
 performed continuously by the SC at a frequency of approximately 1 Hz. Before the
 beginning of each treatment, if the expected elements are correctly installed and the
 detector parameters are within the expected range, the SC communicates to the
 Supervision System (SS) the grant for delivery.

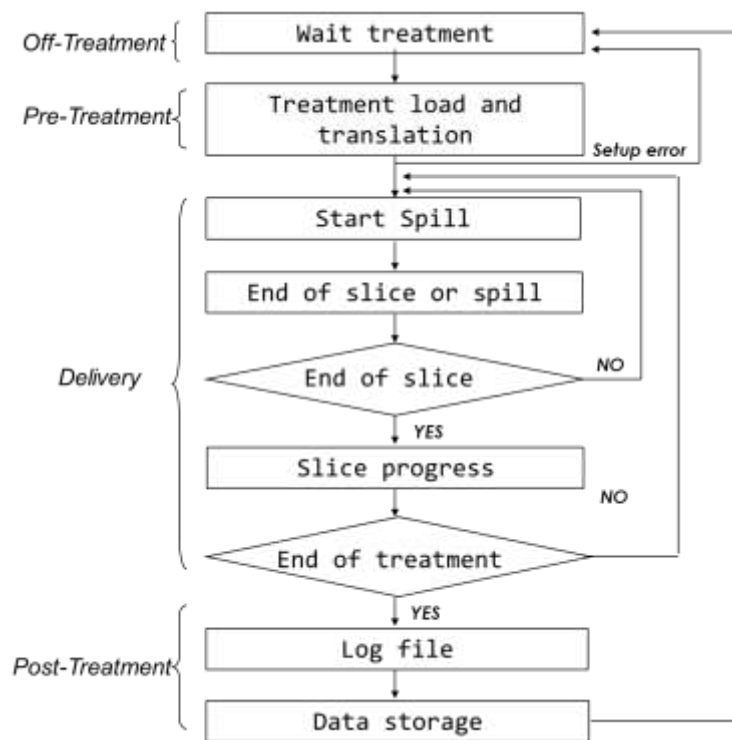
340 III.C DDS tasks and operations

In the DDS several tasks are running in parallel, each performing different operations.
 The list of tasks, subdivided in six main groups, is shown in Table 2.

DDS task groups					
Input data management	Treatment delivery	Output data management	Interlocks management	Data publishing	Detector management
Passive element readout and check	Accelerator synchronization	Treatment <i>Log</i> file creation	Interlock signal generation	Data publishing to Supervision System	Gas pressure and temperature check
Treatment file transformation	Beam monitoring and control	<i>Log</i> file to OIS		Data publishing in the local control room	High voltage control
FPGA data creation	Control of the Scanning power supplies	DDS data remote storage			
	DD recovery update				

Tab. 2. List of the major DDS tasks subdivided in 6 groups (columns).

350 The sequence of a treatment can be divided in the four phases indicated in the flowchart of Figure 6. Following this division, the operations performed by the tasks will be described in detail.



355

Fig. 6 Flow chart with the DDS operations.

1) Off treatment.

360 To keep the patient safety to high standards, a large number of system components is continuously checked before treatment delivery. Interlock management, data publishing and detector management are always in operation to issue a warning if any anomalous condition is detected. For example, the *Scan FPGA* sends a pre-configured set of currents to the power supplies of the scanning magnets and receives measured currents

365 and the power supplies status. Furthermore *Int FPGA*, *Strip FPGA* and *Pixel FPGA* continuously read the detectors in order to monitor background.

2) Pre treatment.

Few minutes before treatment, during patient positioning procedures, the Fast Control receives the *DD_Treatment* file via the Treatment Console (TC), as shown in Figure 7. For each spot, the FC performs the conversion of the properties defined by the TPS to the corresponding quantities used internally by the DDS. In detail, number of particles is converted to number of counts read by the integral chambers, the conversion factor being determined daily with the method described in [22], and spot coordinates at the iso-center are converted to beam position in strip units at each strip detector. For the first conversion, the gas temperature and pressure measured by the SC is accounted for. Furthermore the steering magnet currents, corresponding to the required coordinates, are also computed. Spots to be treated with the same energy are grouped in binary files (*Input FPGA* in Figure 7, named *slice_data*, *sld* file), one for each slice. Later during the treatment, data stored in the *sld* files will be sequentially uploaded into the memory boards, spill by spill, to be accessed by the FPGAs of the FC.

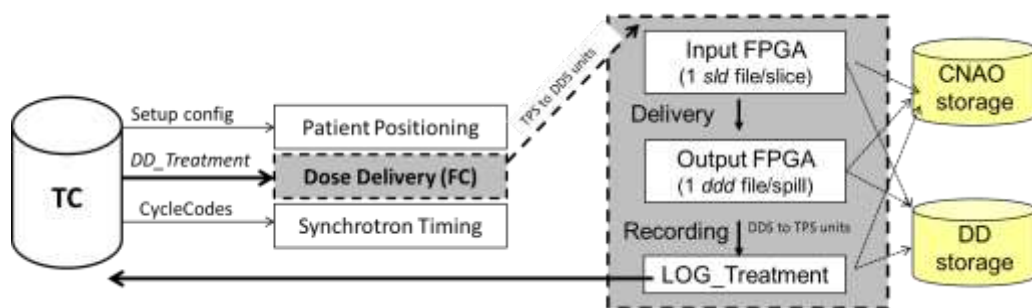


Fig. 7. Data flow during a treatment delivery

385 Detector background, high voltage, gas temperature and pressure, passive elements setup and interlock registers are also checked; if no problem is found, DD moves into a

ready status, which will be acknowledged by the SS in order to deliver the beam. In case of need, the SS can require the DDS to abort the treatment procedure just before irradiation, even if patient is ready and treatment loaded.

390 3) Beam delivery.

Each spill starts after the FC acknowledge of the *cycle_code* (see section III.B.2.1). The MTG triggers the operations which drive the requested beam in the right treatment room. The delivery starts, following the spot sequence defined in the *sld* files. As soon as one of the two integral chambers reaches the prescribed number of counts for a given spot, a trigger from the *Int FPGA* is sent to the *Scan FPGA* which sets the new currents of the scanning magnets. In parallel the same trigger event is received by the *Strip* and *Pixel FPGAs* to load the reference data of the next spot used for the interlock and position feedback. Once the last spot of a slice has been treated (this can take more than one spill as described in Sec. II.B and in Figure 2b) the *Int FPGA* immediately stops the beam delivery by acting on the beam chopper.

At the end of each spill the FC, by means of the *Timing FPGA*, sends a request for a new spill by specifying a *cycle_code* which can coincide or not with the previous one, depending if the slice has been concluded or not. In the latter case, the FC reloads into the memories the data of the current slice, where the spots already delivered with the previous spill have been removed. As shown in Figure 7 FPGA output data, containing the on-line DDS measurements, are temporary stored in the FC controller as a binary file, one for each spill, called *dose_delivery_data (ddd)*. The availability of these files which contain complete beam monitor readout is mandatory for creating the *Log* file.

4) Post Treatment.

410 When the last spot of the last slice is irradiated, a *Log* file is prepared and sent to the OIS which applies further checks against the planned treatment, in order to grant the

end of the dose delivery. A *Log* file is created by FC by using the data stored in the *ddd* files and applying conversions to provide the quantities listed in Tab. 4. Finally the DDS ends the treatment saving *sld* and *ddd* files in a remote storage for off-line data analysis. Such analysis will yield important feedback on the performance of the system as shown in [23] and [24].

Total number of slices in the field
Total number of spots in the field
For each slice: accelerator cycle_code
For each slice: number of spots
For each spot within a slice: number of particles
For each spot within a slice: Spot position (X in mm at isocenter)
For each spot within a slice: Spot position (Y in mm at isocenter)
Total number of particles in the field
Passive element configuration

Tab. 4. Main parameters recorded in the *Log* file.

420 **III.C.1 Interlock management**

The safety of the treatment mainly relies on two interlock systems: Patient Interlock System (PIS) and Safety Interlock System (SIS). These systems collect anomalous or error conditions detected by the equipment components and either force the immediate interruption of the beam delivery or inhibit the operations till the conditions persist.

The PIS is dedicated to the patient safety by acting on the beam chopper to interrupt the treatment when an interlock from any subsystem occurs. The delivery can thus be interrupted for a short time (few seconds) allowing the recovery of the normal treatment execution or can be terminated when the faulty condition causing the interlock persists also after the reset performed by the operator. If this occurs, the treatment is interrupted through a safe recovery procedure where the undelivered dose is calculated by the OIS

based on the number of particles and spots stored in the DD *Log* file and used to provide a new field to be delivered as soon as possible to complete the dose fraction.

All the DDS error conditions are collected and sent to the PIS by means of a hardware
 435 signal, one for each interlock, in order to guarantee fast reaction. Interlocks are generated by the FPGA of FC, SC when the quantities listed in Tables 5 and 6 are outside the tolerance window.

<i>Critical condition (FC)</i>	<i>Tolerance intervals</i>
QInt1-QInt2	< 100
(QInt1-QInt2)/QInt1	>10%
Beam intensity (protons)	< 3×10^{10} protons/s
Beam intensity (C ions)	< 5×10^8 C ions/s
Spot position deviation in X	< 2 mm
Spot position deviation in Y	< 2 mm
Mismatch in Cycle_code	--

440 Tab. 5. List of the main Fast Control interlocks with tolerance intervals in use. QInt1 and QInt2 are the number of counts measured by the integral chambers Int1 and Int2 respectively.

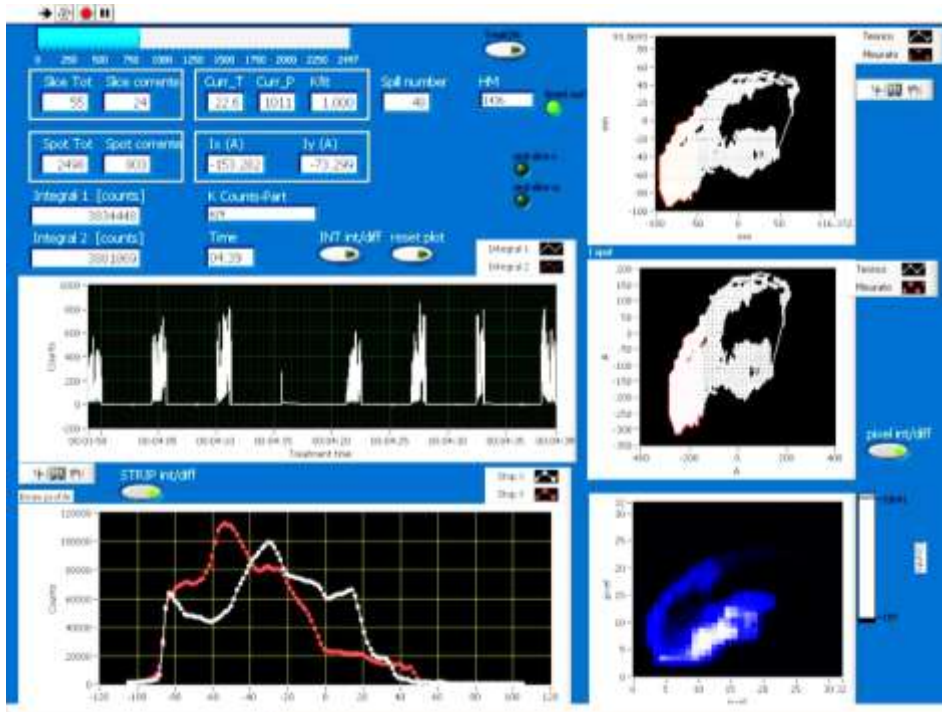
<i>Critical condition (SC)</i>	<i>Tolerance intervals</i>
Gas temperature (BOX1 and BOX2)	$16^{\circ}\text{C} < T < 26^{\circ}\text{C}$
Gas pressure (BOX1 and BOX2)	$9 \times 10^4 \text{ Pa} < P < 11 \times 10^4 \text{ Pa}$
HV (BOX1 and BOX2)	$395 \text{ V} < HV < 405 \text{ V}$

445 Tab. 6. List of the main Slow Control interlocks with the tolerance intervals in use for
BOX1 and BOX2

One battery backed-up device, called Dose Delivered Recovery system (DDR), continuously receives, stores and displays the last treated slice and spot of each slice
450 during irradiation. It can work for at least 20 minutes without external power supply and in case of major system fault occurring during a treatment it will retain important information.

III.C.2 Data publishing

455 Each treatment room is provided with its own Local Control Room (LCR), where all the remote operations related to the treatment execution are managed. A program has been setup, which receives from the FC and displays measured data, system status and treatment progress. In the DDS monitor display the beam position, the number of
monitor counts and the percentage of delivered spots and slices delivered are
460 continuously updated. If any interlock occurs, the display will show it allowing to quickly pinpoint the problem which stops the beam. A snapshot of the DDS monitor display during a carbon ion treatment is shown in Figure 8.



465 Fig. 8. Snapshot of the DDS monitor display where monitor read-out data are published
continuously. Data shown refer to a carbon ion treatment.

The status of the DDS during the *Off*, *Pre* and *Post* treatment phases is also monitored by the Supervision System (SS) and displayed in the main control room.

470 Figure 9 summarizes all the described interfaces used by the FC and SC to perform the
DDS tasks together with the type of data exchanged.

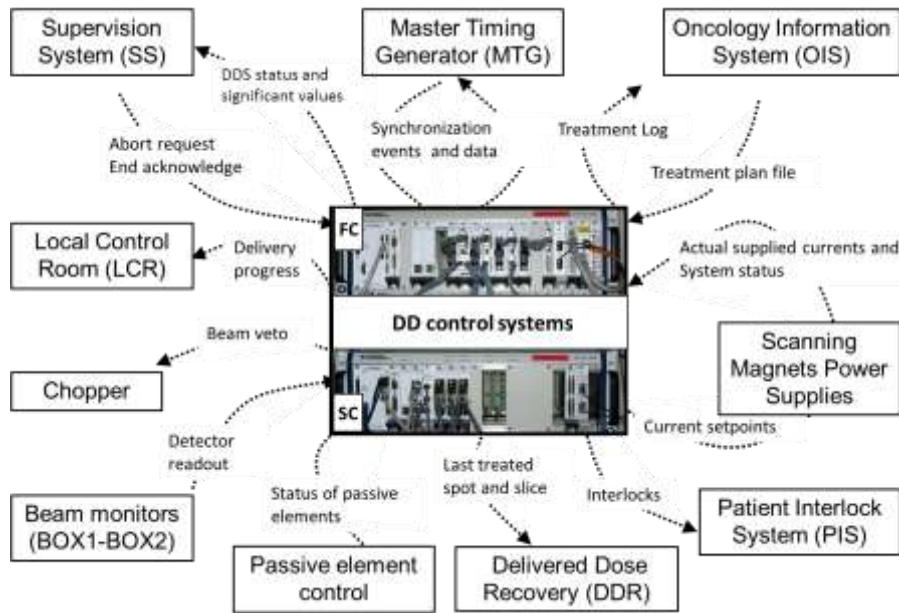


Fig. 9. FC and SC interfaces with the main exchanged data: MTG, OIS, Scanning PSs,
 475 PIS, Chopper, LCR and SS are external systems while beam monitors, passive elements
 and DDR are DDS subsystems.

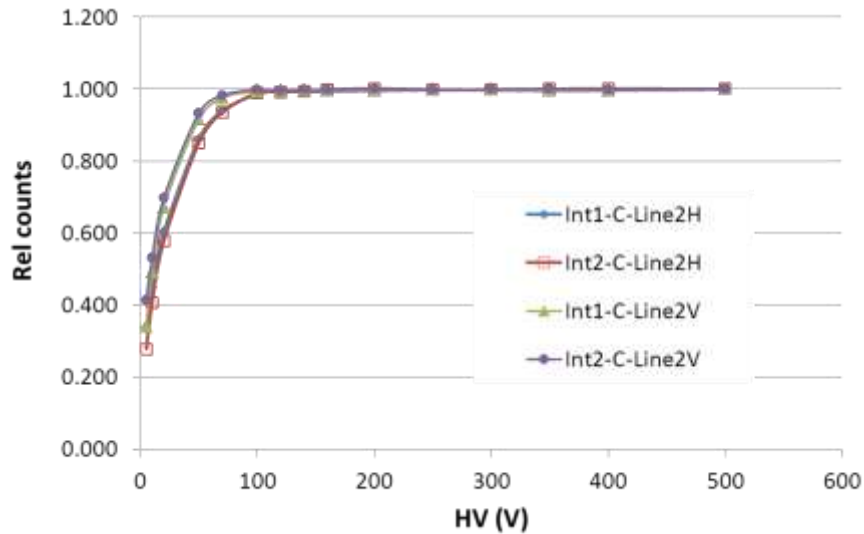
IV. ACCEPTANCE TESTS

The DDS acceptance tests have been performed at CNAO during pre-clinical beam
 480 commissioning phase and results were found to satisfy the requirements. Although
 detailed description of the accuracy and the performance of the system are out of the
 scope of this work and will be reported in a separate paper, few examples are presented
 here to show the main characteristics of the DDS: the integral chambers collection
 efficiency and gain uniformity are followed by a uniform square dose distribution
 485 delivered at the isocenter plane.

IV. A. Charge collection efficiency

The integral chambers efficiency is regularly checked to verify the stability of the
 charge collected under identical irradiation conditions both with protons and carbon
 490 ions. Example of efficiency measurement in the two beam lines (room 2, horizontal and

vertical lines) are shown in Figure 10, where the number of counts measured by Int1 and Int2 as a function of the applied high voltage in the range 50 to 500 V is presented normalized to the measurement at 500 V.



495

Fig. 10. Relative number of counts measured by Int1 and Int2 with high voltage ranging from 50 to 500 V for two beam lines (room 2, horizontal and vertical lines) when carbon ions are delivered with $E = 300\text{MeV/u}$ and beam intensity $I = 10^8$ particles per second. Data are normalized to the counts acquired at 500V.

500

The results show that, at a voltage exceeding 150 V the efficiency saturates; at the nominal operating voltage of 400 V an efficiency of 99.99 % is achieved.

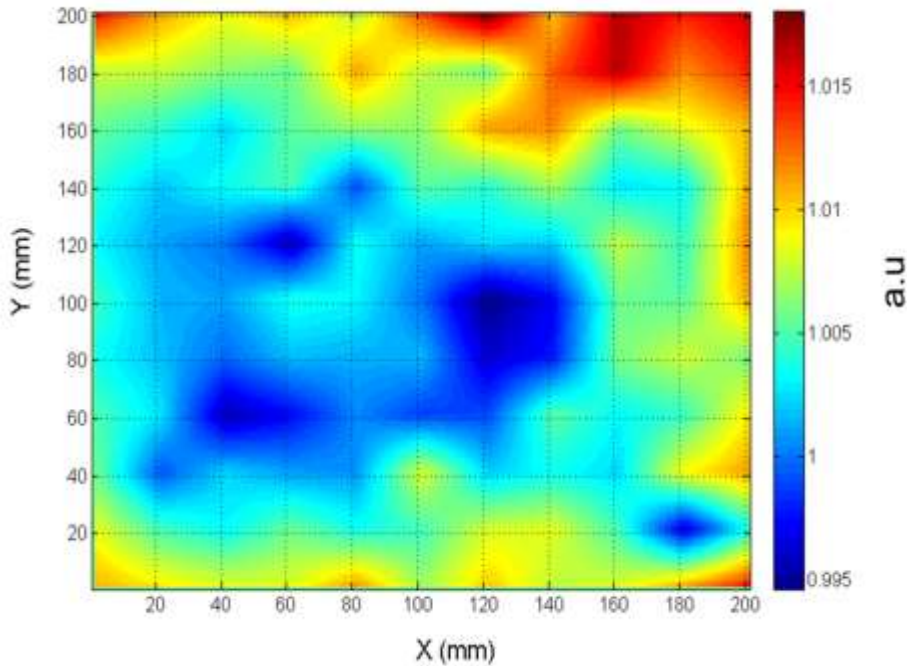
IV.B. Gain uniformity of the integral chambers

505

In order to test the 2D gain uniformity of the integral chambers, a 7×7 square grid of spots, spaced 26 mm each other was delivered. The charge collected by an external ionization chamber (PTW T34080) put in air at the isocenter, moved spot by spot synchronously with the beam, was used as a reference to measure the relative gain in each point. The gain was found to be uniform within $\pm 1.5\%$, for all the chambers in

510

use. A Lagrange interpolation on a 1 mm grid was used to obtain a $200 \times 200 \text{ mm}^2$ gain distribution grid shown in Figure 11 which is used by the DDS to apply fine non-uniformity corrections to the monitor counts.



515

Fig. 11 Example of 2D gain distribution of an integral chamber.

IV.C. Dose Distributions

520 2D uniform fields are periodically delivered for medical physics quality assurance tests by irradiating a regular grid spots in air at the isocenter, each spot with the same number of particles. Square fields of $150 \times 150 \text{ mm}^2$ size with spot spacing of 3 mm (protons) and 2 mm (carbon ions) are delivered for different beam lines, particles and energies. The dose uniformity of the delivered fields is measured by using EBT3 radiochromic
525 films. Figure 12 shows a film on the left and the corresponding absolute dose profiles along main axis and diagonals on the right. The uniformity is evaluated in terms of flatness, $(I_{\text{max}} - I_{\text{min}}) / (I_{\text{max}} + I_{\text{min}})$. Results from different beam lines, particles and

energies are found to be within the tolerance in use at CNAO of 5% within the 80% of the field size (70% for diagonals).

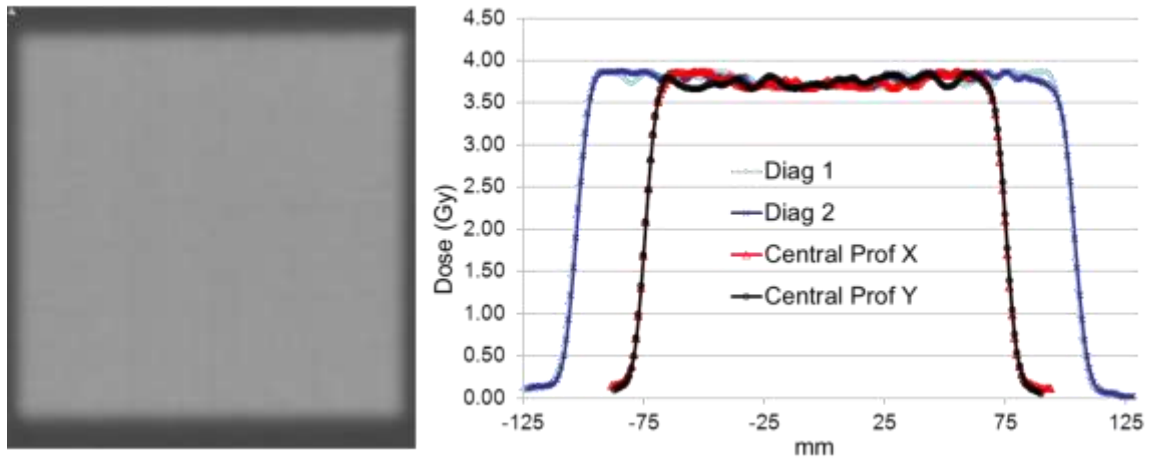


Fig. 12. Example of radiochromic film irradiated with a proton beam: on the left a 150 x 150 mm² square field in air at the isocenter is shown while on the right the measured dose profiles along main axes (x and y) and diagonals are presented.

535 V. DISCUSSION

The design of the DDS described in this paper started ten years ago with a prototype of the beam monitor chambers, fully tested on the GSI clinical carbon ion beams [25].

The system reported here consists of two components: the beam monitors (BOX1 and BOX2) and the DDS control system. The established clinical protocols and the expected
540 beam characteristics as fluence, shape and delivery time structure have been taken into account to define the system requirements. The technical specifications were driven by the clinical requirements compatibly with the present technological limitations. The guidelines included the accuracy in beam steering and in flux measuring at a high
545 scale integration to achieve a high frequency, deadtime free readout of hundreds of channels with uniform behavior that reduces the need of a cross-calibration. The system

was built to operate permanently, reading out the detectors and receiving trigger events continuously.

Particular care was devoted to patient safety, which lead to the design of a patient safety
550 interlock system to timely detect potential hazards as they develop and to trigger the
immediate stop of the irradiation.

The current system is well optimized for the treatment of static tumors. However it has
been designed to allow enough flexibility to implement tracking, gating or repainting
555 techniques to treat tumors in moving organs [26, 27, 28].

The ability of the DDS to accomplish a safe and accurate treatment was validated during
the commissioning phase, some examples being reported in this paper. The high level
of reliability and robustness has been verified in two years of activity with 100% of
system up-time. In these years the DDS has rarely needed more than regular
560 maintenance.

The careful analysis of the DDS data provided a thorough understanding of the
performance of the system and stability in time. Typically the number of particles
delivered in each spot was found to differ from the prescribed one by less than 1% in
more than 95% of the spots. Additionally, in over 90% of the spots the beam position
565 was found to differ less than 1 mm. These results were found to be largely independent
from the field shapes and in a wide range of number of particles per spot.

Several tests of the treatment recovery procedure were performed using dose
measurements in phantom to verify the consistency of the dose for treatments where
abnormal terminations have been forced (i.e. partial treatment delivery followed by
570 treatment recovery managed by the OIS) leading to negligible deviations from the
prescribed dose.

Daily checks of the conversion factors used to convert the number of particles into monitor counts are performed at CNAO for each treatment line and for protons and carbon ions separately. The results are found to be always within $\pm 2\%$, with a negligible dependence on the beam intensity.

VI. CONCLUSIONS

The Dose Delivery System, specifically designed, developed and now in use in the clinical routine of CNAO, is described. It implements the pencil beam scanning technique with protons and carbon ions and, so far, has been used to treat more than 200 patients. This system has been proven to guide and control the therapeutic pencil beams with a high level of reliability, reaching performances well above clinical standards in terms of dose accuracy and stability. Examples of the system performance are reported in this work.

The interest in the technical details described in this paper is particularly relevant since the number of facilities treating patients with the pencil beam scanning technique is increasing worldwide.

ACKNOWLEDGMENTS

The authors wish to acknowledge the designers and all the technical staff of CNAO, INFN and University of Torino who contributed to the development of the Dose Delivery System in the past ten years. A special thank to Marco Lavagno of De.Tec.Tor for the strong help in the installation and commissioning of the system.

The authors wish to acknowledge Ugo Amaldi for the fundamental role in the birth of CNAO and Sandro Rossi for his leadership and advice during the entire span of the CNAO project.

600

REFERENCES

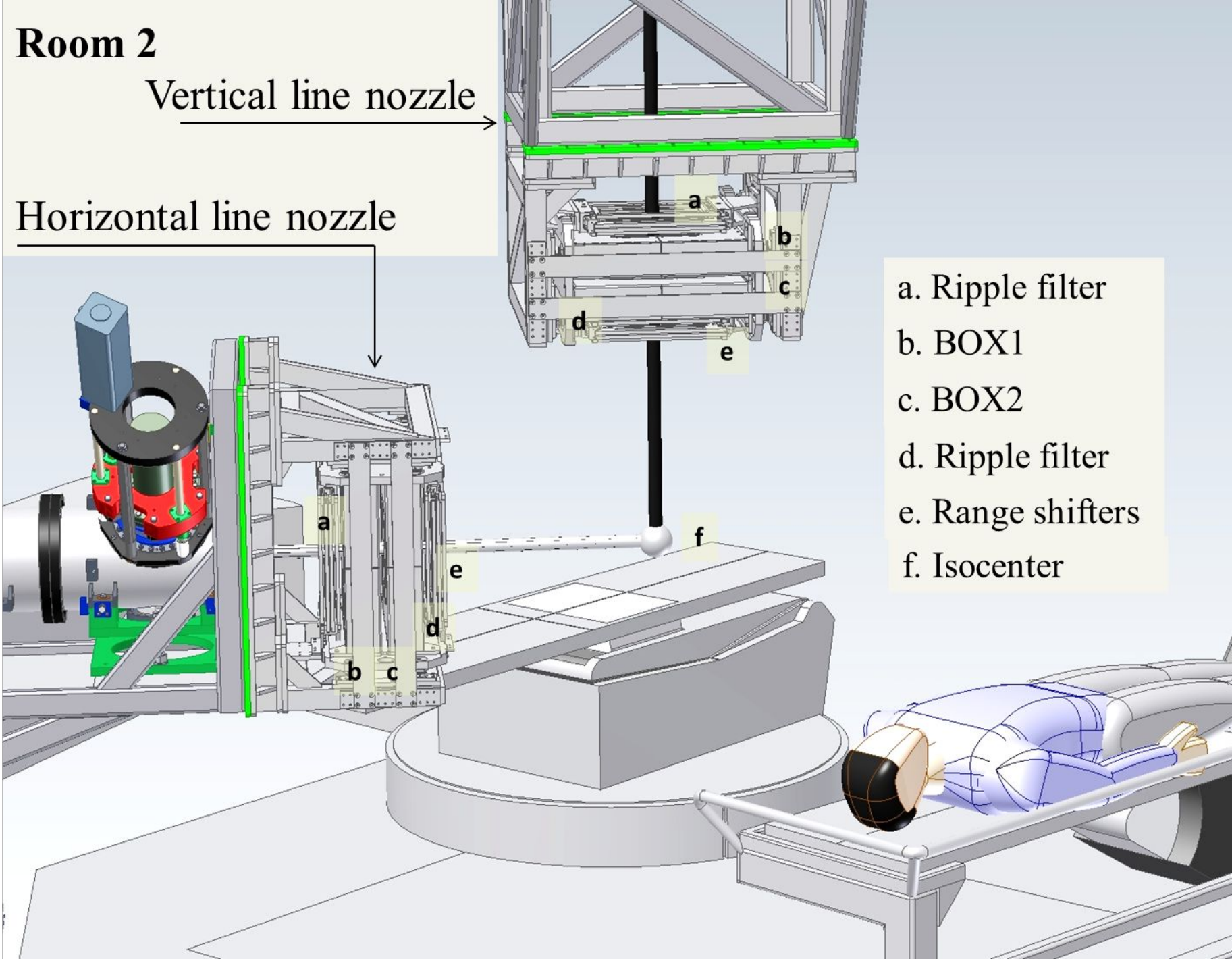
- [1] A.M. Koehler, R.J. Schneider, J.M. Sisterson “Flattening of proton dose distributions for large field radiotherapy” *Med. Phys.* 4 (4), 297-301 (1977)
- 605 [2] E. Grusell, A. Montelius, A. Brahme, G. Rikner, K. Russell “A general solution to charged particle beam flattening using an optimized dual-scattering-foil technique, with application to proton therapy beams” *Phys. Med. Biol.* 39 (12), 2201-2216 (1994)
- [3] A.J. Wroe, R.W. Schulte, S. Barnes, G. McAuley, J.D. Slater, J.M. Slater “Proton beam scattering system optimization for clinical and research applications” *Med. Phys.* 610 40 (4), (2013)
- [4] T. Kanai, K. Kawachi, Y. Kumamoto, H. Ogawa, T. Yamada, H. Matsuzawa, T. Inada “Spot scanning system for proton radiotherapy” *Med. Phys.* 7 (4), 365-369 (1980)
- [5] T. Haberer, W. Becher, D. Schardt, G. Kraft “Magnetic scanning system for heavy ion therapy” *Nucl. Instr. Meth A* 330, 296-305 (1993)
- 615 [6] E. Pedroni, R. Bacher, H. Blattmann, T. Bohringer, A. Coray, A. Lomax, S. Lin, (...), A. Tourovsky “The 200-MeV proton therapy project at the Paul Scherrer Institute: Conceptual design and practical realization” *Med. Phys.* 22 (1), 37-53 (1995)
- [7] D. Schardt and T. Elsasser, D. Schulz-Ertner “Heavy-ion tumor therapy: Physical and radiobiological benefits” *Reviews of modern physics*, Vol. 82 (1)/383(43) (2010)
- 620 [8] A. Smith, M. T. Gillin, M. Bues, X. R. Zhu, K. Suzuki, R. Mohan, S. Woo, A. Lee, R. Komaki, and J. Cox, “The M. D. Anderson protontherapy system,” *Med. Phys.* 36, 4068–4083, (2009)
- [9] T. Furukawa, T. Inaniwa, S. Sato, T. Shirai, Y. Takei, E. Takeshita, K. Mizushima, Y. Iwata, T. Himukai, S. Mori, S. Fukuda, S. Minohara, E. Takada, T. Murakami, K. 625 Noda, “Performance of the NIRS fast scanning system for heavy-ion radiotherapy” *Med. Phys.* (37), 11, 5672-5682, (2010)
- [10] S.E. Combs, O. Jäkel, T. Haberer, J. Debus “Particle therapy at the Heidelberg Ion Therapy Center (HIT) - Integrated research-driven university-hospital-based radiation oncology service in Heidelberg, Germany” *Radiot. and Oncol.* 95, (1), 41-44,(2010)
- 630 [11] M. Benedikt, A. Wrulich “MedAustron-project overview and status”, *Eur. Phys. J. Plus*, 126 (7), 1-11, (2011)
- [12] M. Schippers, J.M., Lomax, A.J. “Emerging technologies in proton therapy“ *Acta Oncologica*, 50 (6), 838-850 (2011)
- [13] Particle Therapy Co-Operative group homepage. <http://www.ptcog.ch/>
- 635 [14] S. Rossi “The status of CNAO” *Eur. Phys. J. Plus* 126, 78 (2011)
- [15] S. Molinelli, A. Mairani, A. Mirandola, G. Vilches Freixas, T. Tessonier, S. Giordanengo, K. Parodi, M. Ciocca and R. Orecchia “Dosimetric accuracy assessment of a treatment plan verification system for scanned proton beam radiotherapy: one-year experimental results and Monte Carlo analysis of the involved uncertainties” *Phys. Med. Biol.* 58, 3837–3847(2013)
- 640

- [16] P. Fossati, S. Molinelli, N. Matsufuji, M. Ciocca, A. Mirandola, A. Mairani, J. Mizoe, A. Hasegawa, R. Imai, T. C. Kamada, R. Orecchia, H. Tsujii, “Dose prescription in carbon ion radiotherapy: A planning study to compare NIRS and LEM approaches with a clinically-oriented strategy” *Phys. Med. Biol.* 57, 7543-7554 (2012)
- 645 [17] U. Weber, G. Kraft, “Design and construction of a ripple filter for a smoothed depth dose distribution in conformal particle therapy” *Phys. Med. Biol.*, 44 (11), 2765-2775 (1999)
- [18] F. Bourhaleb, A. Attili, R. Cirio, G.A.P. Cirrone, F. Marchetto, M. Donetti, M. A. Garella, S. Giordanengo, N. Givchchi, S. Iliescu, A. La Rosa, J. Pardo, A. Pecka, C. Peroni “Monte Carlo simulations of ripple filters designed for proton and carbon ion beams in hadrontherapy with active scanning technique” *Journal of Physics: Conference Series*, 102, 1, (2008)
- 650 [19] M. Krämer, O. Jakel, T. Haberer, G. Kraft, D. Schardt and U. Weber “Treatment planning for heavy-ion radiotherapy: physical beam model and dose optimization” *Phys. Med. Biol.* 45, 3299-3317 (2000)
- 655 [20] S. Giordanengo, M. Donetti, F. Marchetto, A. Ansarinejad, A. Attili, F. Bourhaleb, F. Burini, R. Cirio, P. Fabbriatore, F. Voelker, M.A. Garella, M. Incurvati, V. Monaco, J. Pardo, C. Peroni, G. Russo, R. Sacchi, G. Taddia, A. Zampieri “Performances of the scanning system for the CNAO center of oncological hadron therapy” *Nucl. Instr. Meth. A* 613, 317, (2010)
- 660 [21] S. Giordanengo, M. Donetti, M. A. Garella, F. Marchetto, G. Alampi, A. Ansarinejad, V. Monaco, M. Mucchi, I. A. Pecka, C. Peroni, R. Sacchi, M. Scalise, C. Tomba, R. Cirio, “Design and characterization of the beam monitor detectors of the Italian National Center of Oncological Hadron-therapy (CNAO)”, *Nucl. Instr. Meth. A* 698 202-207, (2013)
- 665 [22] O. Jakel, G. H. Hartmann, C. P. Karger, P. Heeg and S. Vatnitsky “A calibration procedure for beam monitors in a scanned beam of heavy charged particles” *Med. Phys.* 31, 5, (2004)
- [23] H. Li, N. Sahoo, F. Poenisch, K. Suzuki, Y. Li, X. Li, and X. Zhang, Andrew K. Lee, M. T. Gillin and X. R. Zhu “Use of treatment log files in spot scanning proton therapy as part of patient-specific quality assurance” *Med. Phys.* 40 (2), 021703, (2013)
- 670 [24] T. Furukawa, T. Inaniwa, Y. Hara, K. Mizushima, T. Shirai, and K. Noda, “Patient-specific QA and delivery verification of scanned ion beam at NIRS-HIMAC”, *Med. Phys.* 40, 121707, (2013)
- 675 [25] R. Bonin, A. Boriani, F. Bourhaleb, R. Cirio, M. Donetti, E. Garelli, S. Giordanengo, F. Marchetto, C. Peroni, C.J. Sanz Freire, L. Simonetti “A pixel chamber to monitor the beam performances in hadron therapy” *NIM A* 519, 674-686, (2004)
- [26] C. Bert and M. Durante “Motion in radiotherapy: particle therapy” *Phys. Med. Biol.* 56 R113, (2011)
- 680 [27] M. Seregni, R. Kaderka, G. Fattori, M. Riboldi, A. Pella, A. Constantinescu, N. Saito, M. Durante, P. Cerveri, C. Bert and G. Baroni “Tumor tracking based on correlation models in scanned ion beam therapy: an experimental study” *Phys. Med. Biol.* 58, 4659–4678, (2013)
- 685 [28] Zenklusen, S.M., Pedroni, E., Meer, D. “A study on repainting strategies for treating moderately moving targets with proton pencil beam scanning at the new gantry 2 at PSI” *Phys. Med. Biol.* 55 (17), 5103-5121 (2010)

Room 2

Vertical line nozzle

Horizontal line nozzle



a. Ripple filter

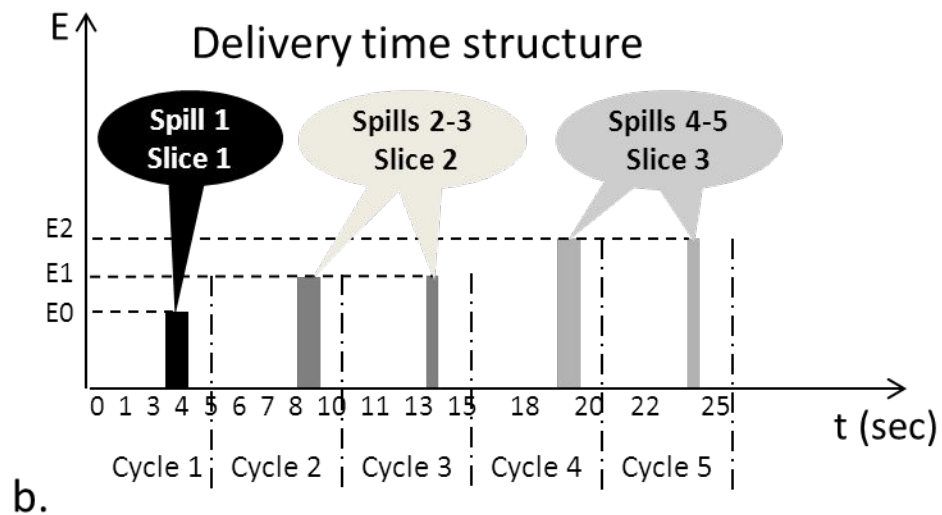
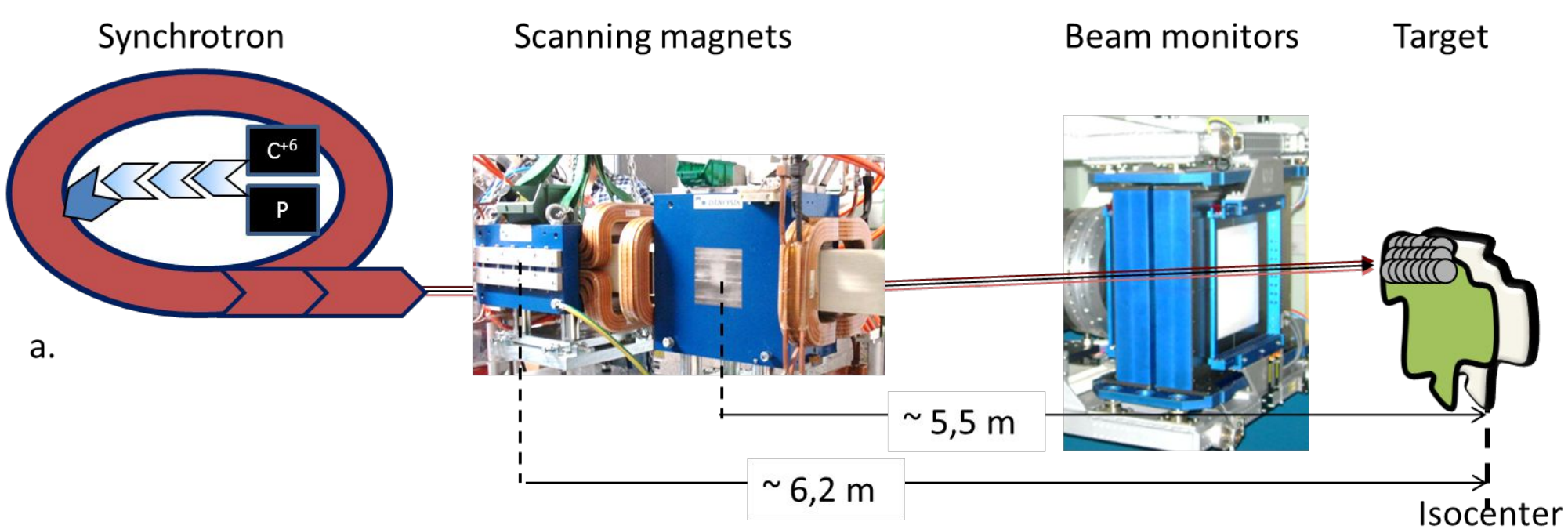
b. BOX1

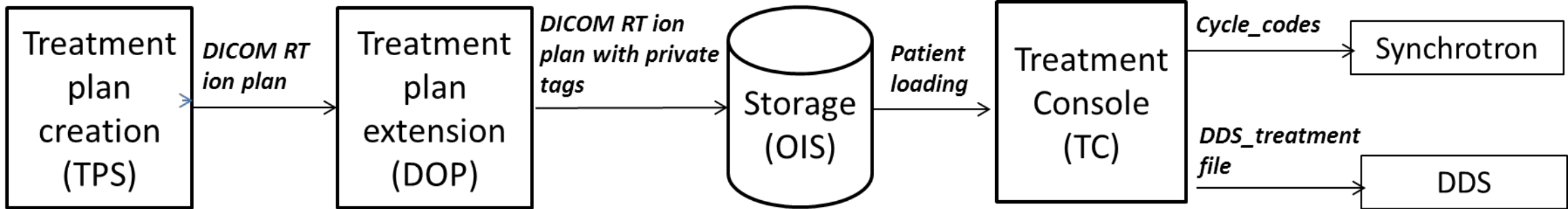
c. BOX2

d. Ripple filter

e. Range shifters

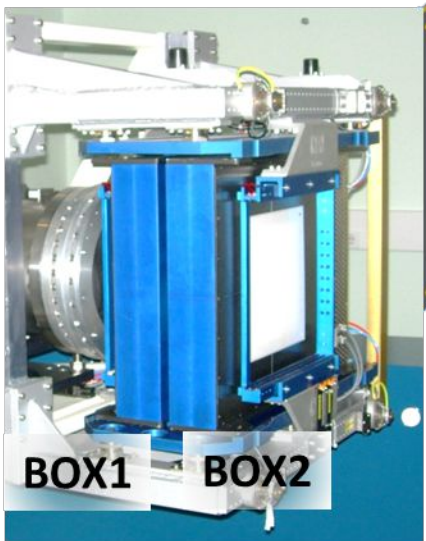
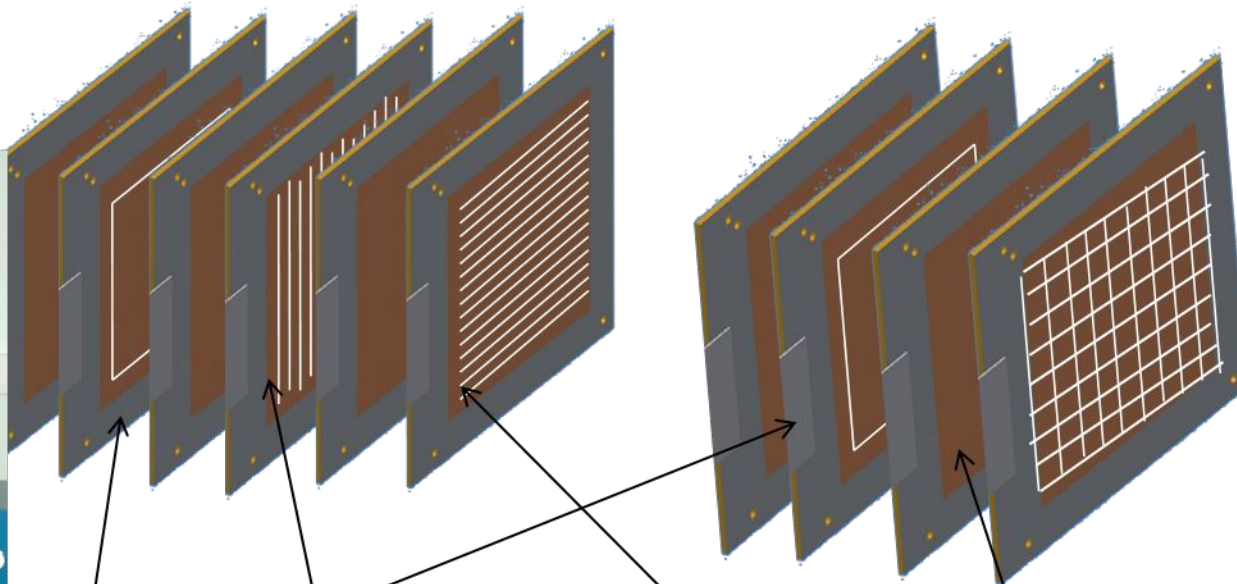
f. Isocenter





BOX1

BOX2



Integral chambers
Sensitive area
24x24 cm²

128 V strips
Strip X
pitch 1.65 mm

128 H strips
Strip Y
pitch 1.65 mm

1024 pixels
Pitch 6.6 mm

Strip and Pixel sensitive area 21x21 cm²



Power supplies of BOX1 and BOX2

Delivered Dose Recovery

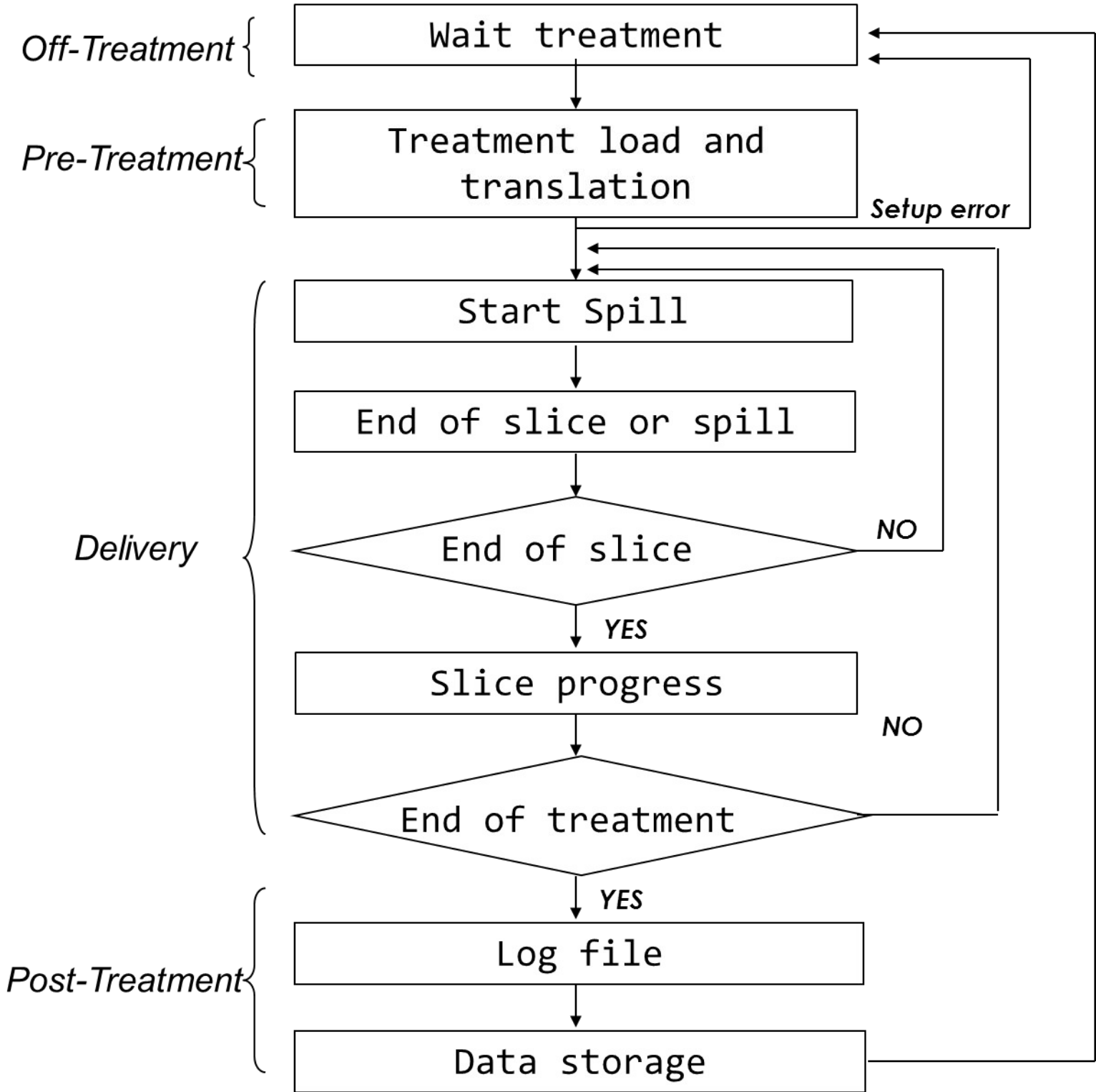
Interlock Interface Modules

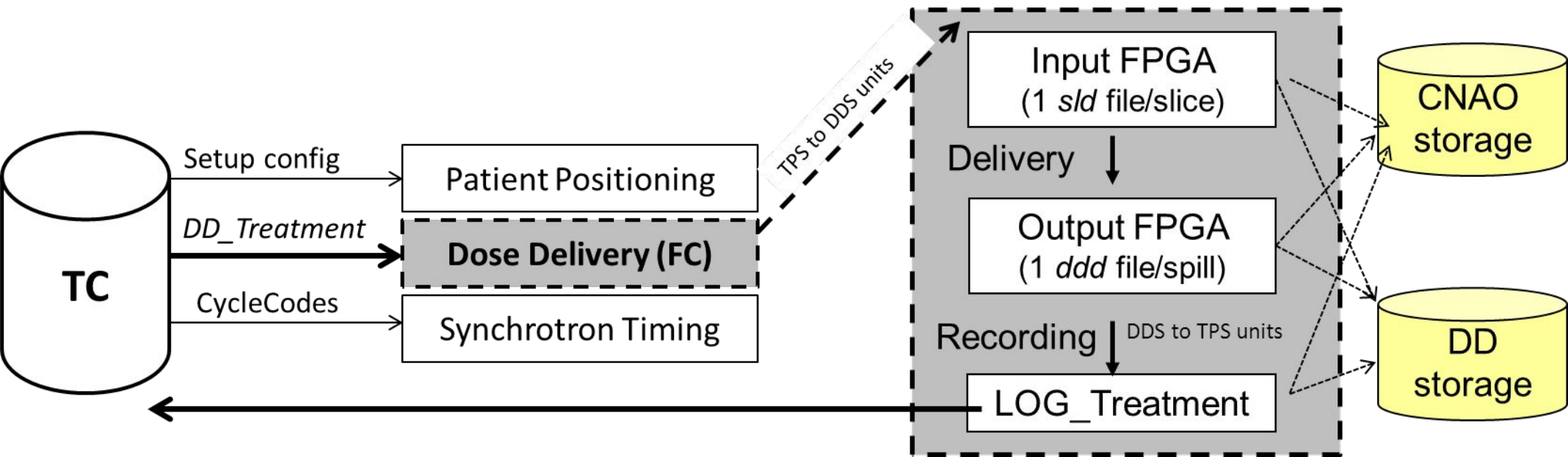
Fast Control PXI crate

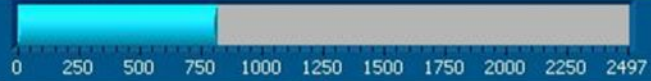
Detector front-end interface

Slow Control PXI crate

Detector gas distribution







Slice Tot: 55
Slice corrente: 24

Curr_T: 22.6
Curr_P: 1011
Kfit: 1.000

Spill number: 48

HM: 1436

Spot Tot: 2498
Spot corrente: 803

Ix (A): -153.282
Iy (A): -73.299

Integral 1 [counts]: 3834448

K Counts-Part: 629

Integral 2 [counts]: 3881869

Time: 04:39

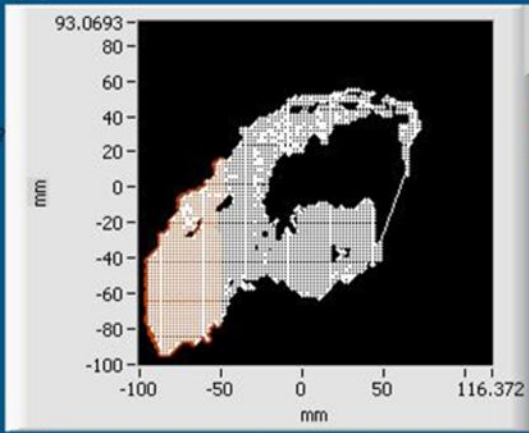
INT int/diff reset plot

Integral 1
Integral 2

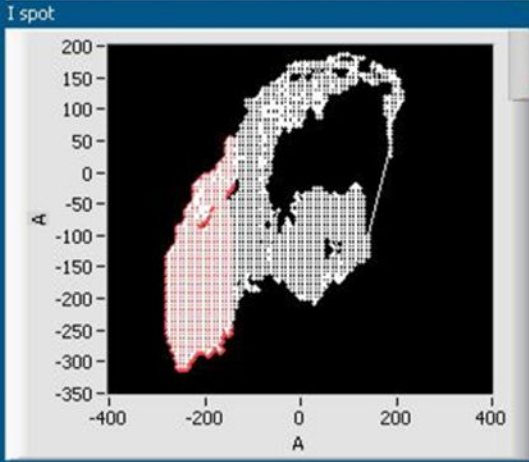


end slice s
end slice sc

timed out?

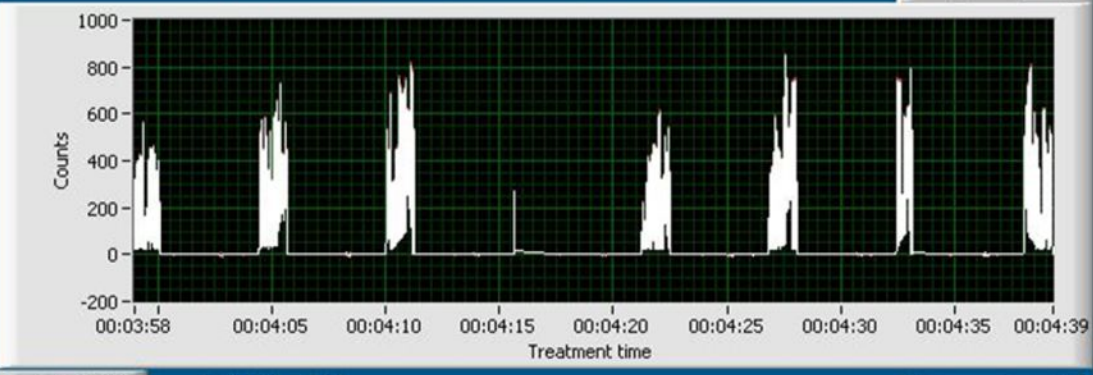


Teorico
Misurato

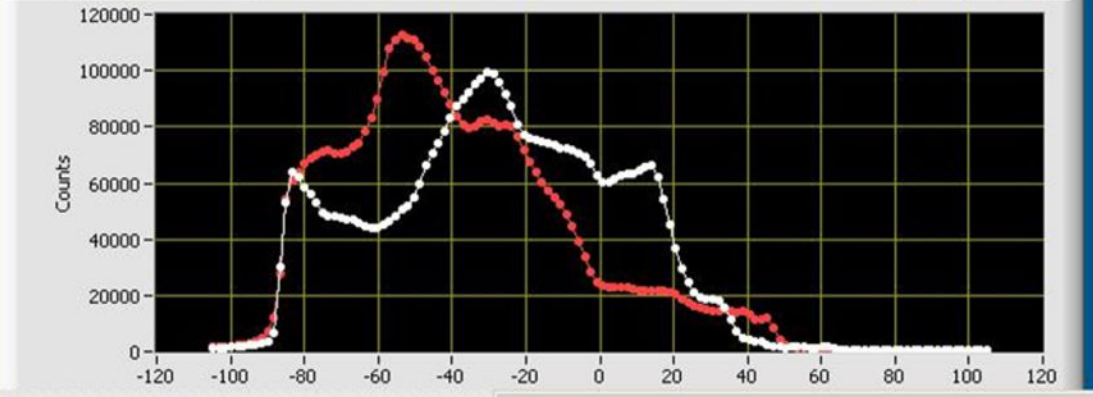


Teorico
Misurato

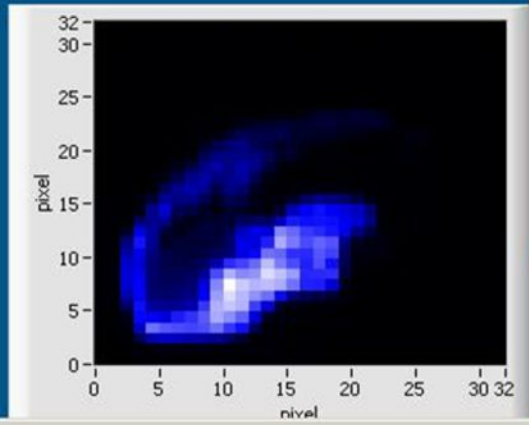
pixel int/diff



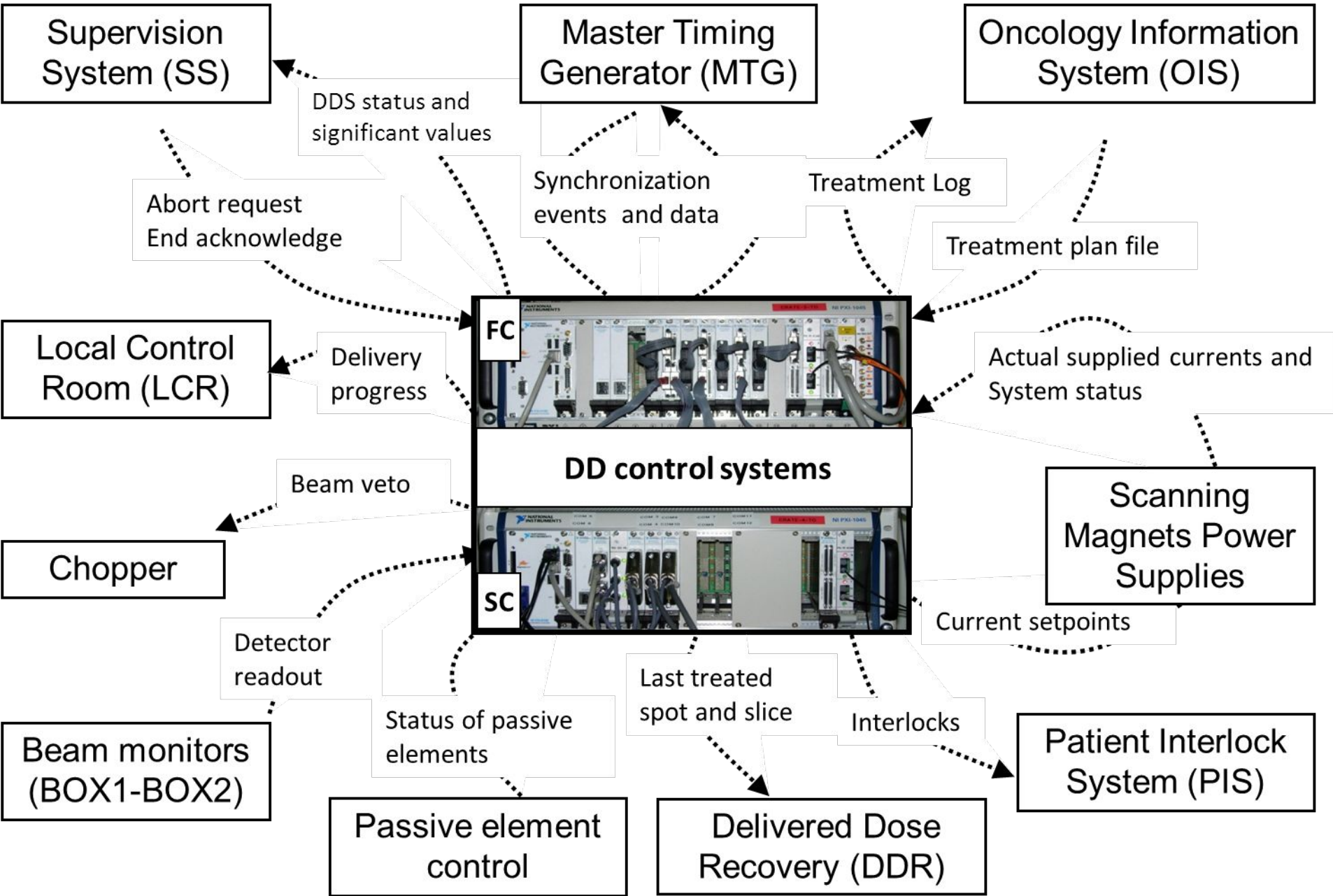
STRIP int/diff



Strip X
Strip Y



Counts: 33641
197



Rel counts

